Research Article | Vol. 13, No. 6 / 1 Jun 2023 / Optical Materials Express 1640
Optical Materials EXPRESS

Theoretical model of an electrically tunable liquid-crystal-based contact lens

O. Sova,[1] T. J. Sluckin,[2] S. Kaur,[3] H. F. Gleeson,[3] and V. Reshetnyak[1,3,*]

[1]Physics Faculty, Taras Shevchenko National University of Kyiv, Volodymyrska Street 64/13, Kyiv 01601, Ukraine
[2]School of Mathematical Sciences, University of Southampton, SO17 1BJ, UK
[3]School of Physics and Astronomy, University of Leeds, LS2 9JT, UK
*victor.reshetnyak@gmail.com

Abstract: Milton, et al. [Opt. Express **22**, 8035 (2014)] have constructed a model electronic liquid crystal contact lens for the correction of presbyopia. This paper constructs a theoretical model for this lens. Good agreement between theory and experimental data is achieved, although the indications are that the precise parameters of the lens differ slightly from those prescribed by the designers of the lens. We discuss the temperature dependence of the optical power, the sensitivity of the device to manufacturing process and the properties of such lenses containing a number of different known liquid crystals. The model can be used for engineering optimization of the existing prototype.

1. Introduction

Presbyopia is an age-related disease which affects vision acuity. In the light of rapidly ageing populations, there is an increasing need for efficient and cheap treatments of this condition. Current treatments include presbyopia surgery, GRIN (graded index) lenses or multiple sets of correction glasses. The alternative approach of contact lenses has numerous advantages, enabling the wearer to maintain an active lifestyle which may be less inhibited than if wearing spectacles. However, contact lenses are less suitable in contexts where efficient vision requires rapid changes between optical powers.

Milton et al. [1–4] have suggested that tunable LC contact lenses may be a solution to this problem. This device should enable a person to perform near-vision tasks (e.g. reading, working on computer, etc.) with lenses switched on, while far-vision tasks (e.g. driving) are carried out using lenses in the safe unpowered mode.

In a more general context, a number of different tunable LC lens designs have been suggested over the last decade. All use spatially shaped electric fields to control director reorientation and thus the effective refractive index of the system. By changing the applied voltage, it is then possible to change the optical power of the lens. For example, non-planar electrodes [5] or optically hidden dielectric layers [6] can be used to induce a parabolic refractive index distribution, so that planar LC layers act as an ordinary GRIN lens. The common problem of these designs is that they require relatively high operation voltages. This does not inhibit, for example, smartphone or web camera applications. But the close proximity to the human eye required by contact lenses, and the sensitivity of the eye to electric fields, renders these designs unsuitable for contact lens use. Several reviews of the field have recently been published [7,8].

This paper presents a theoretical model of the LC contact lens discussed by Milton et al. [1], which operates at a low working voltage (the threshold is ~0.7 V_{rms}). We have considered the case of a cylindrical two-dimensional lens with strong surface anchoring. A full three dimensional model would be more realistic, but it is a rather challenging task that requires considerably deeper theoretical analysis.

#491405 https://doi.org/10.1364/OME.491405
Journal © 2023 Received 22 Mar 2023; revised 22 Apr 2023; accepted 22 Apr 2023; published 12 May 2023

Optical Materials EXPRESS

We have compared the predictions of our model to experimental results. The model is rather successful. It thus can be fruitfully extended to make predictions about the properties of different kinds of lenses. Specifically, we discuss the properties of a lens in which the active material is a high birefringence LC replacing the 5CB LC (pentyl-cyanobiphenyl) used experimentally. We have also investigated the dependence of the optical power of the lens on temperature and geometry. Consequently our model can be used for engineering optimization of the existing prototype.

The plan of the paper is as follows. In section 2 we remind the reader of the details the lens design introduced by Milton et al. [1]. In section 3, we present the details of the model. In section 4, we present the results of our calculations. In section 5, we discuss our results and present some brief conclusions.

2. Device description

The electrically tunable liquid crystal (LC) contact lens (CL) under consideration has been discussed by Milton et al. [1]. In order to make this paper self-contained, we reproduce the basic features here. A plan is shown in Fig. 1. The lens consists of two mated plastic (PMMA, $n_{PMMA} = 1.49$ [9]) lenses. Between them is a cavity, which is filled with a LC (5CB). In order to simplify the numerical calculations, we work with a two-dimensional cylindrical lens, rather than a three dimensional spherical lens. This approach was used in related previous work [10] and proved to be reliable for modelling liquid crystal lenses.

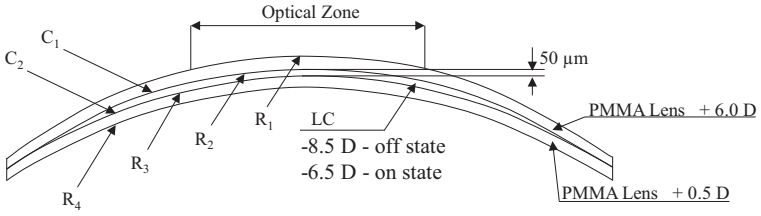

Fig. 1. Schematic representation of the LC lens. R_1-R_4 are the radii of curvature of the lenses. C_1 and C_2 are the liquid crystal layer boundaries. The lens dimensions are appropriate for an average-sized eye. Electrodes are placed directly onto the boundaries C_1, C_2; this reduces the control voltage required for on-off switching. The LC layer is sandwiched between lenses made from poly(methyl acrylate) (PMMA), which is a common material used in the contact lens industry.

The tunability of the lens lies in the liquid crystal director reorientation, which takes place in xOz plane, as shown in Fig. 2. We suppose strong planar anchoring at both plastic surfaces of the LC lens coated with orientation layers, with the director in the xOz plane.

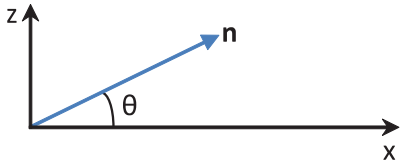

Fig. 2. Director reorientation.

Optical Materials EXPRESS

3. Theory

3.1. Optics

When an external voltage is applied, the director in the LC cell reorients in the limit that it completely aligns with the electric field (true, strictly speaking, only in the high field limit and with straight cell geometry). The refractive index changes from values close to n_e, when the lens is unpowered, to values close to n_o. We suppose the incident light to be polarized in the reorientation plane. A more detailed analysis, provided below, also includes the curved shape of the lens, and the elasticity of the liquid crystal. The power of the lens is a function of the difference between the optical path lengths at different points of the lens. Thus changing the refractive index enables the optical power of the device to be tuned [1, 6, 10]. The total optical power (OP) in the device consists of contributions from the upper and lower plastic lenses, as well as from the tunable LC lens, and can be described as follows:

$$OP = OP_{PMMA\ top} + OP_{PMMA\ bottom} + OP_{LC}. \tag{1}$$

The optical powers of the upper and lower plastic lenses can be calculated using the thin lens approximation [11]:

$$\begin{aligned} OP_{PMMA\ top} &= \frac{1}{f} = (n_{PMMA} - 1)\left[\frac{1}{R_1} - \frac{1}{R_2}\right], \\ OP_{PMMA\ bottom} &= \frac{1}{f} = (n_{PMMA} - 1)\left[\frac{1}{R_3} - \frac{1}{R_4}\right]. \end{aligned} \tag{2}$$

The optical power of the LC lens can be calculated using the following formula [12,13].

$$OP_{LC} = \frac{\lambda}{\pi R_0^2}[(\varphi(0) + \Delta(0)) - (\varphi(R_0) + \Delta(R_0))], \tag{3}$$

where $(\varphi(0)+\Delta(0))$ is the optical phase retardation in LC (see eq.(4) below) and air (where Δ is defined similarly to φ in Eq. (4), but for the case of $n_{eff} = n_{air}$) respectively, that would occur in the middle of the optical zone, while $(\varphi(R_0)+\Delta(R_0))$ is the analogous quantity at the edge of the optical zone. However, we note that the correction for the refractive index of air as compared to that of a vacuum is very small; we assume $n_{air} \approx 1$, and the radius of optical zone $R_0 = 2$ mm. The optical retardation φ is calculated using the standard formula [10,14,15]

$$\varphi = \frac{2\pi}{\lambda}\int n_{eff}(x, z)dz, \tag{4}$$

with the effective refractive index n_{eff} [16] defined by

$$n_{eff} = \frac{n_o n_e}{(n_e^2 \sin^2\theta + n_o^2 \cos^2\theta)^{\frac{1}{2}}}. \tag{5}$$

3.2. Free energy and director reorientation

To describe switching of the liquid crystal lens, we follow the procedure of Sova et al. [10] and Subota et al. [15]. The expression for the free energy of the liquid crystal in the lens is:

$$F = F_{elastic} + F_{electric}, \tag{6}$$

where

$$\begin{aligned} F_{elastic} = &\frac{1}{2}K_{11}\int (\mathrm{div}\,\mathbf{n})^2 dV + \frac{1}{2}K_{22}\int (\mathbf{n}\cdot\mathrm{curl}\,\mathbf{n})^2 dV \\ &+ \frac{1}{2}K_{33}\int [\mathbf{n}\times\mathrm{curl}\,\mathbf{n}]^2 dV \end{aligned} \tag{7}$$

Optical Materials EXPRESS

is the elastic free energy of the director field. The electrostatic contribution to the free energy is:

$$F_{electric} = -\frac{1}{2}\int (\mathbf{E}\cdot\mathbf{D})dV, \tag{8}$$

where $\mathbf{D}$ is the electric displacement vector.

Minimizing the free energy functional gives rise to the following Euler-Lagrange equation:

$$\begin{aligned}\theta_{xx}(K_{11}\sin^2\theta + K_{33}\cos^2\theta) + \theta_{zz}(K_{11}\cos^2\theta + K_{33}\sin^2\theta)+\\ +(K_{33}-K_{11})[(\theta_z^2-\theta_x^2)\sin\theta\cos\theta + \theta_{xz}\sin 2\theta + \theta_x\theta_z\cos 2\theta]+\\ +\varepsilon_0\varepsilon_a(\sin\theta\cos\theta(E_z^2-E_x^2) + E_xE_z\cos 2\theta) = 0,\end{aligned} \tag{9}$$

subject to strong anchoring boundary conditions

$$\begin{cases}\theta(C_1) = \theta_1\\ \theta(C_2) = \theta_2\end{cases}, \tag{10}$$

and where θ_1, θ_2 are the pretilt angles prescribed by the curvatures C_1 and C_2 on the top and bottom surfaces of the liquid crystal layer (see Fig. 1).

The equation for the electric field potential is obtained from Maxwell's electrostatics equations

$$\begin{aligned}\operatorname{div}\mathbf{D} &= \rho\\ \operatorname{curl}\mathbf{E} &= 0.\end{aligned} \tag{11}$$

Assuming that there are no free charges in the LC, Eq. (11) can be rewritten as

$$\nabla(\tilde{\varepsilon}\varepsilon_0\nabla U) = 0, \tag{12}$$

where $\tilde{\varepsilon}\varepsilon_0 = \hat{\varepsilon}\varepsilon_0 + i\frac{\sigma}{\omega}$, where $\hat{\varepsilon}$ is the permittivity tensor, ω is the electric field frequency, σ is the electric conductivity of the liquid crystal and $U = U_{re} + iU_{im}$ is the electric potential (where U_{re} and U_{im} are respectively the real and imaginary parts).

The permittivity tensor $\hat{\varepsilon}$ is given by:

$$\hat{\varepsilon} = \begin{pmatrix}\varepsilon_\perp + \varepsilon_a\cos^2\theta & 0 & \varepsilon_a\cos\theta\sin\theta\\ 0 & \varepsilon_\perp & 0\\ \varepsilon_a\cos\theta\sin\theta & 0 & \varepsilon_\perp + \varepsilon_a\sin^2\theta\end{pmatrix}. \tag{13}$$

Equation (12) can then be recast as the following set of equations

$$\begin{cases}\nabla(\hat{\varepsilon}\varepsilon_0\nabla U_{re}) - \frac{\sigma}{\omega}\nabla^2 U_{im} = 0\\ \nabla(\hat{\varepsilon}\varepsilon_0\nabla U_{im}) + \frac{\sigma}{\omega}\nabla^2 U_{re} = 0\end{cases}. \tag{14}$$

Combining Eqs. (9) and (14) yields a coupled system of partial differential equations:

$$\begin{aligned}\theta_{xx}(K_{11}\sin^2\theta + K_{33}\cos^2\theta) + \theta_{zz}(K_{11}\cos^2\theta + K_{33}\sin^2\theta)+\\ +(K_{33}-K_{11})[(\theta_z^2-\theta_x^2)\sin\theta\cos\theta + \theta_{xz}\sin 2\theta + \theta_x\theta_z\cos 2\theta]+,\\ +\varepsilon_0\varepsilon_a(\sin\theta\cos\theta(\mathrm{E}_z^2-\mathrm{E}_x^2) + \mathrm{E}_x\mathrm{E}_z\cos 2\theta) = 0\end{aligned} \tag{15a}$$

Optical Materials EXPRESS

$$\begin{cases} \nabla(\hat{\varepsilon}\varepsilon_0\nabla U_{re}) - \frac{\sigma}{\omega}\nabla^2 U_{im} = 0 \\ \nabla(\hat{\varepsilon}\varepsilon_0\nabla U_{im}) + \frac{\sigma}{\omega}\nabla^2 U_{re} = 0 \end{cases} . \tag{15b}$$

This system of equations has been solved numerically, using the COMSOL-Matlab environment [17,18], with the following boundary conditions:

$$\begin{cases} \theta(C_1) = \theta_1 \\ \theta(C_2) = \theta_2 \end{cases} , \quad \begin{cases} U(C_1) = U_0 \\ U(C_2) = 0 \end{cases} . \tag{16}$$

3.3. Modelling details

Here we note two points, one concerned with the lens parameters, and one concerned with the nematic configuration. With regard to the lens parameters, systematic differences between the observed and calculated optical powers suggest that the experimentally defined lens parameters are only approximate. In order to optimize the comparison between theory and experiment, some fitting is necessary. When this fitting is carried out, good agreement between theory and experiment is achieved. Parameter details for the specific apparatus used in the experiments [1] are listed in Table 1.

Table 1. Apparatus parameters

Parameters	Experimenter best value	Optimized value
R_1	7.7 mm	(not optimized)
R_2	8.5 mm	9.11 mm
R_3	7.9 mm	7.86 mm
R_4	7.8 mm	7.92 mm
Upper PMMA layer central thickness	100 µm	(not optimized)
LC layer central thickness	50 µm	(not optimized)
Lower PMMA layer central thickness	100 µm	(not optimized)
n_e	1.71	1.729

The parameters used for fitting were R_2 - R_4 and n_e. As we can see from Table 1, the bottom plastic lens was intended to be a negative one. However, measurements of optical powers before assembly suggest that the lens radii differed slightly from their anticipated values. For our primary simulations, the radius R_4 was adjusted, in such a way that the total OP of the lower lens remains equal to +0.5 D. The optimization procedure outlined below was then used for fitting. Specifically, R_2, R_3, and n_e were used as actual fitting parameters, while R_4 was calculated using the assumption that the OP of the lower lens remained unchanged after the lens had been assembled. The parametric fitting was carried out using the Nelder-Mead optimization algorithm [19,20, Appendix A]. We have also made several assumptions that allow to simplify calculations and decrease computation time. Figure 3 depicts our simulation strategy:

The calculations will show that even small changes in the LC cell radii can significantly alter the optical powers arising from both the LC layer and from the plastic lenses. By way of example, we find that a 5% increase in R_2 at 0 V leads to a 60% change in optical power. Further discussion of these effects is given in section 4.5. As a consequence they carry a significant influence on the total optical power of the device. The result of this extreme sensitivity to the lens parameters is that the fitting process is quite challenging. We have obtained optimal R_2 - R_4 and n_e, which all lie within 7% of the experimental values. A further engineering consequence is that even small differences from the design parameters can result in quite big changes in the optical performance.

Optical Materials EXPRESS

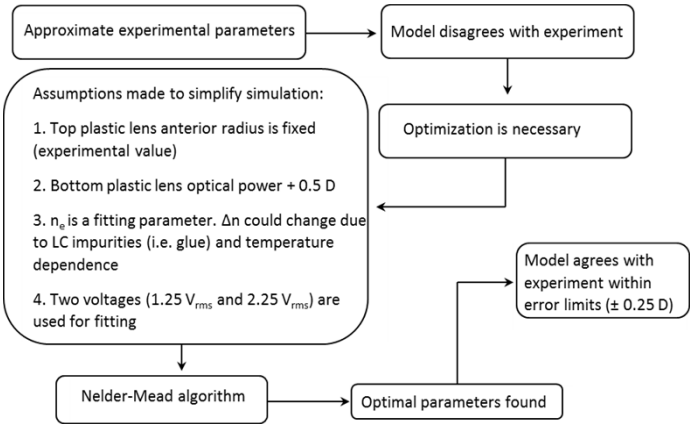

Fig. 3. General modelling strategy description.

We now turn to the nematic configuration. If this is assumed to be cylindrically symmetric, calculation of the optical power requires only that half the device be modeled. However, we note that in Fig. 4 below, this assumption will be relaxed. The specific reason for the possible lack of symmetry in the lens is as follows.

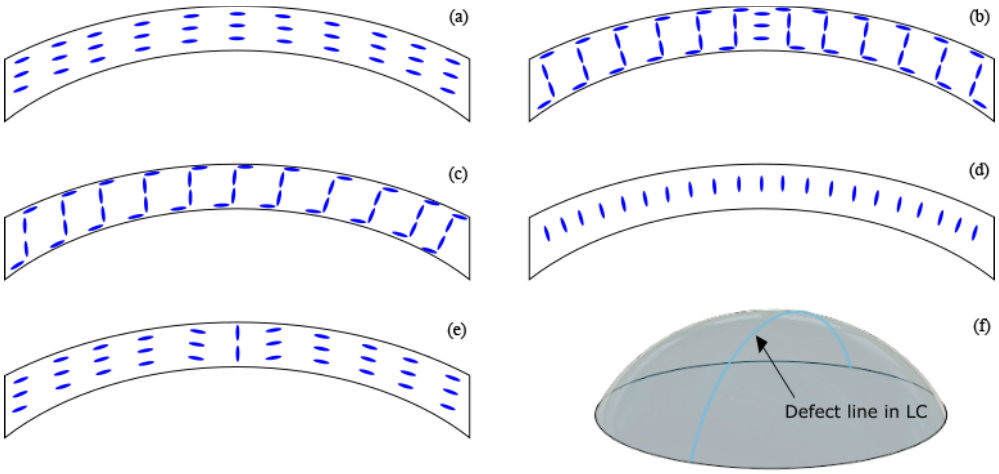

Fig. 4. (a) - Symmetric director distribution at 0 V_{rms}, with orientation governed by boundary conditions. (b) - Symmetric director distribution at 2 V_{rms} containing central defect. (c) - Asymmetric director distribution at 2 V_{rms}. (d) - Lens containing well-oriented liquid crystal without central defect. (e) - Unoriented director distribution containing central defect. (f) - Caricature of optical signature of (e). Note that diagrams (a) to (e) should be regarded as cartoons indicating the basic topology of the calculated configurations, rather than as an accurate representation with particular parameters.

The most likely zero-voltage configuration is that shown in Fig. 4(a). A continuous deformation of this configuration in an applied voltage field is more likely to result in the asymmetric configuration shown in Fig. 4 (c). The symmetric configuration in Fig. 4(b) involves a defect in the center of the lens. In this configuration there is a central region of unoriented nematic, thus corresponding to a higher elastic free energy state than the asymmetric state Fig. 4(c).

Optical Materials EXPRESS

If the oriented state is both defect-free and symmetric, as shown in Fig. 4(d), then the field-free configuration obtained when the voltage is removed will be as shown in Fig. 4(e). But this configuration now contains a defect in the center of the lens. This will then appear like a line across the field of view, as shown in Fig. 4(f).

In what follows we discuss simulations of the symmetric lens, and briefly return to the asymmetric case only in section 5. We use optimized parameters unless stated otherwise.

4. Results

4.1. Director reorientation and electric field

We first note that the shape of the LC cell dictates that, even when no voltage is applied, the director orientation angles at comparable points across the cell differ between the middle and at the edge of the cell. A comparative pictorial representation of the orientation profiles in the on and off states is shown in Fig. 5. This figure depicts director reorientation at several applied voltages, showing that the LC director is voltage-controllable.

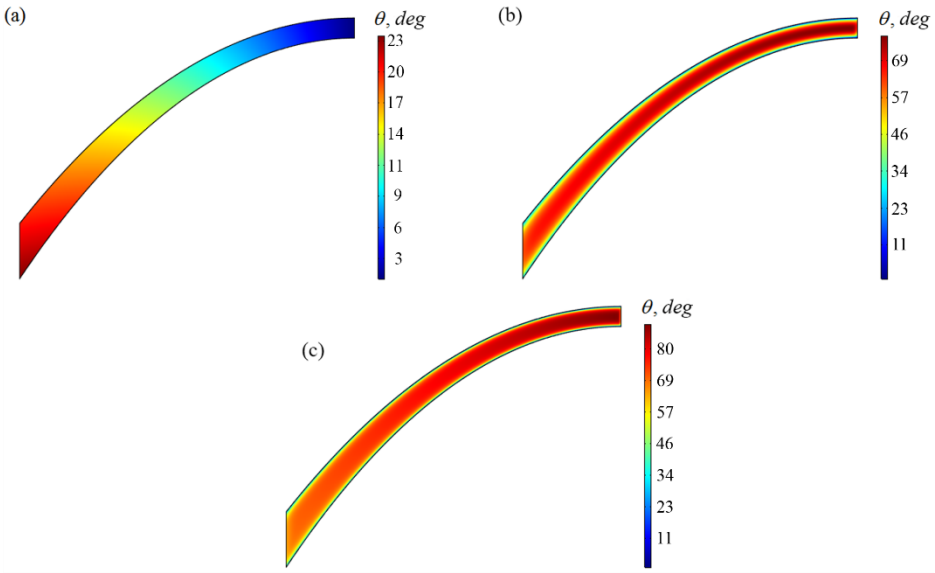

Fig. 5. Director reorientation angle for different applied voltages: (a) 0 V_{rms}; (b) 1.25 V_{rms}; (c) 2.5 V_{rms}.

As a consequence of director reorientation we have voltage-dependent phase retardation, that rises with the increase of control voltage. In Fig. 6 we show the theoretically calculated optical phase retardation (using Eqs. (4) and (5)) as a function of external voltage across the LC layer, where the LC parameters are those of the liquid crystal 5CB.

4.2. Comparison with experiment

In this and subsequent sections, to make comparison with experiment, we use LC physical parameters given in Table 2. We assume that the LC has very low conductivity of $1{\cdot}10^{-15}$ S/m. We first use the theory outlined above to compare with the experiments of Milton et al. [1]. The results of this comparison are shown in Fig. 7. We note that in this comparison we have modified the given lens characteristics in such a way as to optimize the agreement between theory and experiment, following the procedure given in §3.3. The reader can estimate the influence of the parameter optimization from Fig. 8, where modelling results before fitting (using the original

Optical Materials EXPRESS

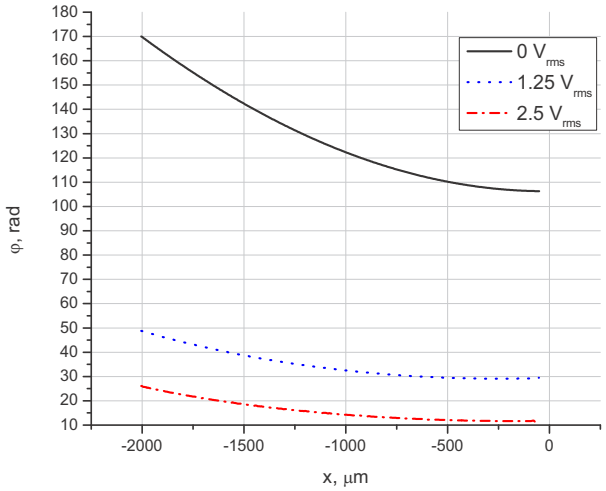

Fig. 6. Optical phase retardation in the LC cell, as a function of distance from the center of the cell x, at various control voltages.

experimental parameters) and after fitting (with optimized lens parameters) are compared with experimental data.

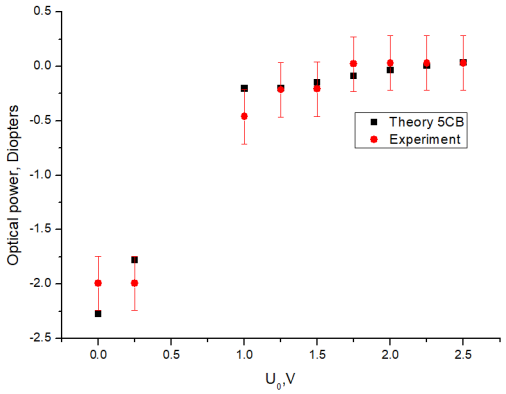

Fig. 7. Voltage dependence of total optical power of lens. Comparison of theory and experiment [1].

We see good agreement between the model with optimal lens characteristics and the experimental data, which proves fitting significance. The change in optical power between on and off states $\Delta_{OP} = OP(V=2)\text{-}OP(V=0)$ is approximately 2 ± 0.25 diopters (using Eqs. (1)–(3)). At voltages sufficiently high that the director has reoriented in most of the cell, the optical power remains more or less constant.

There is, however, an intermediate region of voltages (approximately 0.8 $V_{rms} \leq U_0 \leq$ 1.3 V_{rms}), for which the lens functions poorly. Here defects form as part of the switching process, causing scattering [1]. It was not possible to take data in this regime, and no comparison with experiment has thus been attempted. We remark that this regime corresponds to a range of voltages over which the reorientation has only partially occurred; the outside part of the cell

Optical Materials EXPRESS

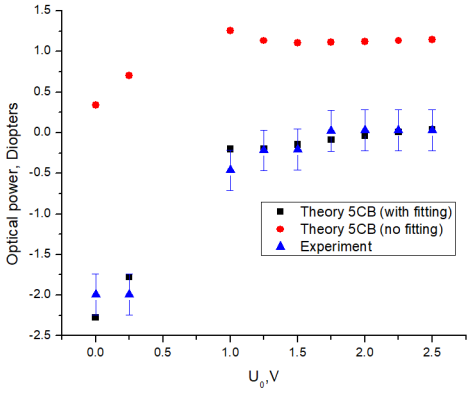

Fig. 8. Voltage dependence of total optical power of lens. Comparison of simulations without fitting, simulations with optimized fitting parameters (see Table 1) and experiment [1].

Table 2. LC parameters used for modelling

Parameters	5CB	E7	E49	W1865
n_o	1.53 [21]	1.52 [22]	1.52 [26]	1.54 [27]
n_e	1.71 [21]	1.73 [22]	1.79 [26]	2.01 [27]
Δn	0.18	0.21	0.27	0.47
K_{ii} (pN): i = 1,3	K_{11} = 4.9 [21] K_{33} = 7.3 [21]	K_{11} = 11.25 [23] K_{33} = 17.8 [24]	K_{11} = 13.76 [26] K_{33} = 23.03 [26]	K_{11} = 10.5 [27] K_{33} = 29.4 [27]
$\varepsilon_{\parallel}$	16.09 [21]	19.54 [25]	21.14 [26]	23.2 [27]
$\varepsilon_{\perp}$	6.02 [21]	5.17 [25]	4.98 [26]	5.0 [27]
λ (nm)	589 [21]	633 [22]	632.8 [26]	589 [27]
ν (kHz)	1 [21]	1	5 [26]	1.5 [27]
T (°C)	25 [21]	25 [22]	25 [26]	25 [27]

has reoriented, whereas the inner part of the cell has not reoriented. It seems likely that a more detailed investigation of the properties of the lens in this regime, including aberration, would also explain this feature of the results. However, such a study goes beyond the scope of this paper.

The comparison with experiment has been quite successful, so we can reasonably ask what the effect of changing some aspects of the system would be.

4.3. Other materials

We first discuss the effect of replacing the 5CB used in the experiment with a number of different liquid crystals. We compare lenses with otherwise identical characteristics, i.e. with best fit parameters corresponding to the experiments modeled in Fig. 7. In Fig. 9 we show the predicted behavior of the optical power of a number of such lenses, as a function of external voltage.

Our results show that one can achieve a bigger optical contrast between low and high voltages by using liquid crystals with higher birefringence. In case of 5CB ($\Delta n = 0.18$) the switch predicted by our theory is approximately 2 diopters, for E7 ($\Delta n = 0.21$) and E49 ($\Delta n = 0.27$) the switch is about 2.3 and 2.9 diopters respectively. But for the LC mixture W1865 ($\Delta n = 0.47$), the switch increases to 5.2 diopters.

Optical Materials EXPRESS

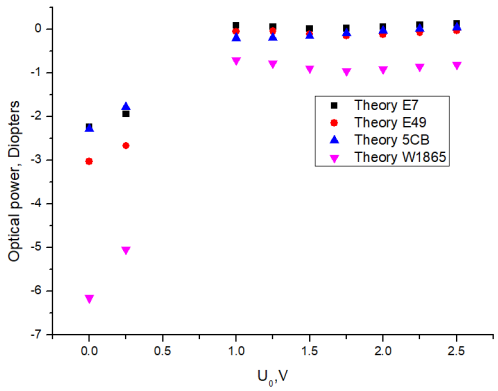

Fig. 9. Theoretical prediction of lens power as a function of voltage for various LCs: E7, E49, 5CB and W1865 LC mixture.

4.4. Temperature dependence

Given that liquid crystal parameters are temperature-dependent, it is important to predict the temperature characteristics of a lens. Here we make such a calculation, in the case of the experimental material 5CB, over the temperature range 25.1°C ≤ T ≤ 33.8°C; we recall that T_{NI} ≈ 35.1°C.

To make specific predictions, it is necessary to describe the temperature dependence of elastic and dielectric properties $\psi = \{K_{11}, K_{33}, \varepsilon_{\perp}, \varepsilon_{\parallel}\}$ of the LC 5CB over this temperature range. We use a parameterization due to Bogi and Faetti [28], who introduced the following set of empirical functions:

$$\psi = A + B(\Delta T - T_o)^{\frac{1}{2}} + C(\Delta T - T_o) + D(\Delta T - T_o)^{\frac{3}{2}}, \tag{17}$$

where $\Delta T = T_{NI}$-T and A, B, C, D, $\mathrm{T_o}$ are the coefficients obtained from the best fit of the experimental data [25].

To parameterize the optical properties of 5CB, we follow Li and Wu [29]:

$$\begin{aligned} n_e(T) &\approx n_i + G'\left(1 - \frac{T}{T_c}\right)^{\beta}, \\ n_o(T) &\approx n_i - \frac{G'}{2}\left(1 - \frac{T}{T_c}\right)^{\beta}, \end{aligned} \tag{18}$$

where β, G' are fitting parameters, and T_c is a temperature close to the clearing temperature. The results of this calculation are shown in Fig. 10. In this figure we concentrate only on the optical powers in the off and on states, noting (see Figs. 7 and 9), that at high voltages, the optical power saturates. We thus consider only two voltages: $U_0 = 0$ $\mathrm{V_{rms}}$, corresponding to the off state, and $U_0 = 2$ $\mathrm{V_{rms}}$, corresponding in all cases to the on-state. The latter voltage is well above the Frederiks threshold and thus in all cases can be regarded as a voltage sufficiently high to align the liquid crystals except in a thin layer close to the surface.

The effect of the temperature increase between 25.1°C and 33.8°C is to decrease the switching optical power significantly. The voltage-induced change in optical power of the lens reaches its minimum value of approximately 1.54 diopters at the highest temperature investigated. Here and in [1] 5CB was used because its parameters are well known and available in the literature. High birefringence LCs (for example E7, E44) whose optical properties are much less temperature-dependent near body temperatures are likely to be more useful in engineering prototypes. Overall,

Optical Materials EXPRESS

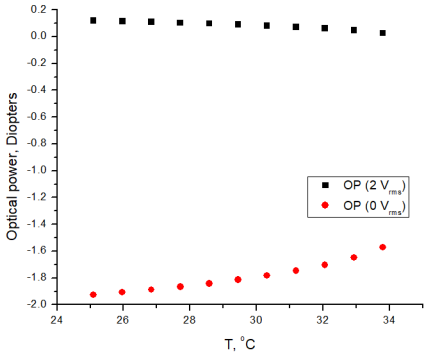

Fig. 10. Lens optical power subject to temperature of 5CB LC ($T_{NI} = 35.1°C$).

however, the tendencies shown in Fig. 10 would remain. We note, however, that the temperature to which the lens is subject also requires careful investigation, as the operating temperature of a contact lens involves a delicate balance between ambient and body temperature.

4.5. Lens deformation

Numerous factors may affect the lens in practice. The experimental process is that parts of the lens are lathed from PMMA blocks and coated with ITO electrodes. Then alignment layers are placed on anterior and posterior surfaces of lower and upper plastic lenses. Next the two lenses are baked together at temperature of about 50°C. The space between plastic lenses is then filled with a LC and finally wires are attached to the device.

One can reasonably assume that at each stage the lens may undergo a variety of deformations. As a consequence, despite the best efforts of experimentalists, some lens parameters may change. Figure 11 shows the response of the optical power of the lens to small relative changes in the LC cell radii, varied within 20% of their initial dimensions.

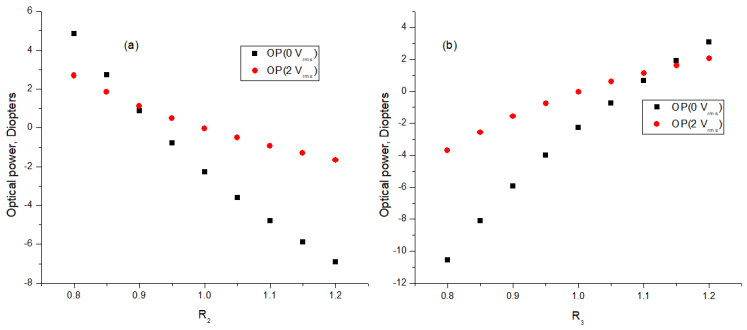

Fig. 11. Optical power as a function of changes in lens curvature: (a) R_2, (b) R_3.

At this point one can conclude that the effect of radii deformation makes a considerable contribution into lens optical power. For instance 5% radii variation causes the optical power to change by more than 1 diopter. This result stresses the importance of precise fabrication methods necessary for lens manufacturing as it is extremely sensitive to deformations.

Optical Materials EXPRESS

5. Discussion and conclusions

We have built a theoretical model of the LC contact lens designed by Milton et al. [1]. The calculations show that the voltage-dependent optical power is very sensitive to lens radii, LC birefringence and other parameters of the system. In particular, simulations with experimental prototype parameters differed considerably from the experimental results. We have discussed possible causes of the uncertainties in the lens parameters. We have then used the Nelder-Mead algorithm to perform parameter optimization. Even though the model is very simplified, using a limited number of optimized fitting parameters, we have achieved good agreement between the theory and the experimental data.

Our simulations also demonstrate that optical phase retardation may change differently in the left and right parts of the lens. The switched configuration then resembles that exhibited in Fig. 4(c). In Fig. 12 we show the optical power dependence on applied voltage, calculated for both left and right halves of the lens. A free energy criterion can be used to predict that one configuration of the system will be preferred to the other. At the same time free energy redistribution takes place when the control voltage changes. This fact requires deeper theoretical analysis and further exploration.

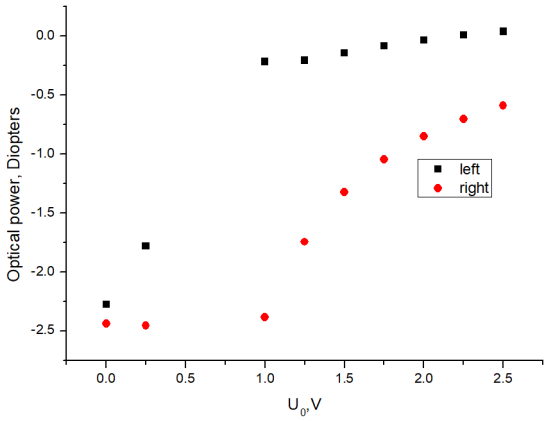

Fig. 12. Optical power of the lens as a function of voltage. Calculations were made separately for left and right parts of the lens using fitting parameters and Eqs. (1)–(3).

Generalizing our results outside the range of the experiments that were carried out, we predict a bigger optical power change between "on" and "off" states using liquid crystals with higher birefringence. The temperature and geometry dependences of LC lens optical power have also been investigated. The study shows that for 5CB cells, increasing temperature over the liquid crystal range $25.1°C < T < 33.8°C$ decreases the induced optical power change, concomitant with the decreasing anisotropy of the liquid crystal system. Given the prediction that lens performance is likely to be significantly influenced by ambient temperature, we suggest that this effect be included in future experiments.

Another aspect explored in the paper is possible deformation of the lens geometry. The theoretical results predict the change in optical power to be extremely sensitive to PMMA lens radii and the shape of the LC cavity. More experimental work should be carried out to ensure lens dimensions are not affected (or affected in accordance with a known pattern) during the assembly process, which is vital for mass production.

Finally, various other factors affecting lens performance during manufacturing have also been discussed. Development of a full three-dimensional model, together with the use of all

Optical Materials EXPRESS

experimental voltages in the optimization process would be a significant improvement of our theory.

Appendix A: optimization using the Nelder-Mead algorithm

The Nelder-Mead method is a simplex numerical method used to find a local minimum or maximum of a function of several variables [19]. A simplex is a generalized triangle with $N+1$ vertices in N dimensional space. We consider optical power to be a function of three variables: R_2, R_3 and n_e. Therefore in our case the simplex is a tetrahedron in three dimensional space of fitting parameters.

The method compares function values at the vertices of the tetrahedron. The worst vertex, where deviation from experimental result is the largest, is replaced with a new vertex. The algorithm creates a sequence of tetrahedrons, the size of each new one is reduced until the stopping criteria is fulfilled and a point in parametric space which corresponds to minimal deviation from experimental data is found. The method is computationally effective.

The optimization was carried out using only experimental data from the two voltages 1.25 V_{rms} and 2.25 V_{rms}. Considerably more computational resources are required if all data points are to be included in the optimization, even if the optimization is restricted to the same set of fitting parameters. Even with this restriction, however, our optimization results succeed in bringing the modelling results much closer to the experimental points.

An important extra feature of our optimization technique involves using boundaries of ±10% of experimental values to set limits for the deviation of the fitting parameters. If at least one of the vertices reached the boundary wall (or all simplex vertices did – flat simplex case) we would regard the results as unreliable. However, in fact this does not occur in our simulations.

Figure 13 gives a description of algorithm's logical decisions [19,20]. The following definitions are introduced to explain the algorithm: $\mathbf{B} = (x_1, y_1, z_1)$ – coordinates of the best vertex (OP is the closest to experiment for this set of fitting parameters), $\mathbf{G} = (x_2, y_2, z_2)$ – coordinates of good vertex (next to the best vertex), $\mathbf{W} = (x_3, y_3, z_3)$ – the worst of four vertices. For these points we have an inequality:

$$f(\mathbf{B}) < f(\mathbf{G}) < f(\mathbf{W}), \tag{A1}$$

where $f(X) = |OP(X) - OP_{experiment}|$ and X is a point in three dimensional parametric space.

$$\begin{aligned} \mathbf{M} &= (\mathbf{B} + \mathbf{G} + \mathbf{W})/3 - \textit{midpoint}, \\ \mathbf{R} &= \mathbf{2} \cdot \mathbf{M} - \mathbf{W} - \textit{reflection point}, \\ \mathbf{E} &= 2 \cdot \mathbf{R} - \mathbf{M} - \textit{extension point}, \\ \mathbf{C} &= (\mathbf{W} + \mathbf{M})/2 - \textit{contraction point}. \end{aligned} \tag{A2}$$

The algorithm is repeated until following condition is satisfied:

$$\begin{aligned} &([OP(\mathbf{B}; 1.25\ V_{\mathbf{rms}}) - OP_{exp.}(1.25\ V_{\mathbf{rms}})]^2 + \\ &[OP(\mathbf{B}; 2.25\ V_{\mathbf{r}ms}) - OP_{exp.}(2.25\ V_{\mathbf{r}ms})]^2)^{\frac{1}{2}} \leq 0.03 \end{aligned} . \tag{A3}$$

Optimal values of R_2, R_3 and n_e were obtained. Comparison with experiment was made using these values. Deviation from experimental data was within experimental error bar limits.

Optical Materials EXPRESS

```
IF f(R)<f(G), THEN Perform Case (i) {either reflect or extend}
              ELSE Perform Case (ii) {either contract or shrink}
BEGIN {Case (i)}                    BEGIN {Case (ii)}
IF f(B)<f(R) THEN                   IF f(R)<f(W) THEN
   replace W with R                    replace W with R
ELSE                                Compute C=(W+M)/2
                                    IF f(C)<f(W) THEN
   Compute E and f(E)                  replace W with C
   IF f(E)<f(B) THEN                ELSE
      replace W with E                 replace W with (B+W)/2
   ELSE                                replace G with (B+G)/2
      replace W with R              ENDIF
   ENDIF                            END {Case (ii)}
ENDIF
END {Case (i)}
```

Fig. A1. Pseudocode for the Nelder-Mead algorithm [20]

A figure of merit for the fit of experiment to theory involves the root-mean-square deviations:

$$RMSD = \sqrt{\frac{\sum_{i=1}^{N} (\mathrm{OP}^{\mathrm{model}} - \mathrm{OP}^{\mathrm{exp}\ eriment})_i^2}{N}} \tag{A4}$$

where N is the number of experimental points. For the model with unoptimized parameters RMSD≈1.63, but with optimized parameters we have RMSD≈0.15 which is much closer to experiment. Thus indeed the optimized parameters provide considerably better agreement with experiment.

Disclosures. The authors declare that there are no conflicts of interest related to this article.

Data availability. Data underlying the results presented in this paper are not publicly available at this time but may be obtained from the authors upon reasonable request.

References

1. H. E. Milton, P. B. Morgan, J. H. Clamp, and H. F. Gleeson, "Electronic liquid crystal contact lenses for the correction of presbyopia," Opt. Express **22**(7), 8035–8040 (2014).
2. H. E. Milton, H. F. Gleeson, P. B. Morgan, and J. H. Clamp, "Switchable liquid crystal contact lenses; dynamic vision for the ageing eye," Proc. SPIE **9004**, 90040H (2014).
3. I. M. Syed, S. Kaur, H. E. Milton, D. Mistry, J. Bailey, P. B. Morgan, J. C. Jones, and H. F. Gleeson, "Novel Switching Mode in a Vertically Aligned Liquid Crystal Contact Lens," Opt. Express **23**(8), 9911–9916 (2015).
4. S. Kaur, Y.-J. Kim, H. Milton, D. Mistry, I. M. Syed, J. Bailey, K. S. Novoselov, J. C. Jones, P. B. Morgan, J. Clamp, and H. F. Gleeson, "Graphene electrodes for adaptive liquid crystal contact lenses," Opt. Express **24**(8), 8782–8787 (2016).
5. S. Subota, V. Yu, H. R. Reshetnyak, and S.-T. Wu, "Tunable-Focus Liquid Crystal Lens with Non-Planar Electrodes," Mol. Cryst. Liq. Cryst. **526**(1), 93–100 (2010).
6. K. Asatryan, V. Presnyakov, A. Tork, A. Zohrabyan, A. Bagramyan, and T. Galstian, "Optical lens with electrically variable focus using an optically hidden dielectric structure," Opt. Express **18**(13), 13981–13992 (2010).
7. Y.-H. Lin, Y.-J. Wang, and V. Reshetnyak, "Liquid crystal lenses with tunable focal length," Liq. Cryst. Rev. **5**(2), 111–143 (2017).
8. J. Bailey, P. B. Morgan, H. F. Gleeson, and J. C. Jones, "Switchable Liquid Crystal Contact Lenses for the Correction of Presbyopia," Crystals **8**(1), 29 (2018).
9. Refractive index and related constants – Poly(methyl methacrylate) (PMMA, Acrylic glass). http://refractiveindex.info.
10. O. Sova, V. Reshetnyak, T. Galstian, and K. Asatryan, "Electrically variable liquid crystal lens based on the dielectric dividing principle," J. Opt. Soc. Am. A **32**(5), 803–808 (2015).
11. M. Born and E. Wolf, *Principles of Optics: Electromagnetic Theory of Propagation, Interference and Diffraction of Light*, 7th Edition, Ch. **IV**, p. 174, (Cambridge University Press, Cambridge, UK, 1999).
12. O. Pishnyak, S. Sato, and O. D. Lavrentovich, "Electrically tunable lens based on a dual-frequency nematic liquid crystal," Appl. Opt. **45**(19), 4576–4582 (2006).

Optical Materials EXPRESS

13. Hongwen Ren and Shin-Tson Wu, "Introduction to Adaptive Lenses," Ch.**VI**, p.199, (John Wiley Sons Inc., United States, 2012).
14. D.S. Goodman, "Geometric optics," in: *Handbook of Optics*, edited by M. Bass, (McGraw-Hill, New York, 1995), Ch. **1**, I.22.
15. S. L. Subota, V. Y. Reshetnyak, S. P. Pavliuchenko, and T. J. Sluckin, "Numerical Modeling of Tunable Liquid-Crystal-Polymer-Network Lens," Mol. Cryst. Liq. Cryst. **489**(1), 366–379 (2008).
16. L. M. Blinov, "Electro-optical effects in liquid crystals," Sov. Phys. Usp. **17**(5), 658–672 (1975).
17. MATLAB R2014a (8.3.0.532) Natick, Massachusetts: The MathWorks Inc., 2014.
18. COMSOL Multiphysics 4.4 (4.4.0.150) COMSOL, Inc., MA, USA, 2013.
19. J. A. Nelder and R. Mead, "A simplex method for function minimization," Comput. J. **7**(4), 308–313 (1965).
20. J. H. Mathews and K. D. Fink, "*Numerical Methods Using Matlab*," 4th Edition, (Upper Saddle River, 2004).
21. Experimental data provided by Dr. Harry Milton, University of Manchester.
22. J. Li, C. H. Wen, S. Gauza, R. Lu, and S. T. Wu, "Refractive indices of liquid crystals for display applications," J. Disp. Technol. **1**(1), 51–61 (2005).
23. Y.-X. Huang and M. Tu, "Dependence of viscoelastic parameters of nematic liquid crystals on pretilt angle and temperature," Curr. Appl. Phys. **10**(2), 561–564 (2010).
24. Y. Zhou and S. Sato, "A method for determining elastic constants of nematic liquid crystals at high electric fields," Jpn. J. Appl. Phys. **36**(7R), 4397–4400 (1997).
25. E. P. Rynes, R. J. A. Tough, and K. A. Davies, "Voltage dependence of the capacitance of a twisted nematic liquid crystal layer," Mol. Cryst. Liq. Cryst. **56**(2), 63–68 (1979).
26. S. Faetti and B. Cocciaro, "Elastic, dielectric and optical constants of the nematic mixture E49," Liq. Cryst. **36**(2), 147–156 (2009).
27. E. Nowinowski-Kruszelnicki, J. Kędzierski, Z. Raszewski, and L. Jaroszewicz, "High birefringence liquid crystal mixtures for electro-optical devices," Opt. Appl. **42**(1), 167 (2012).
28. A. Bogi and S. Faetti, "Elastic, dielectric and optical constants of 4'-pentyl-4-cyanobiphenyl," Liq. Cryst. **28**(5), 729–739 (2001).
29. J. Li and S.-T. Wu, "Extended Cauchy equations for the refractive indices of liquid crystals," J. App. Phys. **95**(3), 896–901 (2004).